Full-Wave Monostatic Radar Cross Section using the Multilevel Fast Multipole Method

Asger Limkilde, Oscar Borries, Peter Meincke, Erik Jørgensen
TICRA
Copenhagen, Denmark
{al,ob,pme,ej}@ticra.com

***Abstract*—An efficient full-wave solver for the computation of monostatic Radar Cross Section (RCS) for electrically large structures using the method of moments is developed. This is accomplished by utilizing higher-order basis functions, to reduce the number of unknowns, and the multilevel fast multipole method, to reduce the computational effort and memory footprint. These techniques are combined with a compression of the right hand sides arising from the different incident angles. We demonstrate that this solver allows for efficient full wave RCS computations of electrically large structures on a laptop.**

***Index Terms*—RCS, MLFMM, Integral Equations**

I. Introduction

The computation of the monostatic Radar Cross Section (RCS) is a critical part of many engineering applications. When considering electrically large structures this has traditionally been done using asymptotic methods [1], [2]. However, in many applications computing an accurate RCS will require solving the problem using a full-wave method. This has until recently been considered too computationally demanding, as the number of unknowns in combination with the potentially large number of incident angles become intractable.

One way to tackle this issue has been by utilizing very advanced and expensive hardware setups to do full-wave RCS computations [3], [4]. Such advanced hardware is necessary when considering full-wave methods based on integral equations such as the Method of Moments (MoM), since it requires $\mathcal{O}(f^6)$ operations.

Acceleration methods, specifically the Multi-Level Fast Multipole Method (MLFMM), have also been investigated [5]. MLFMM scales as $\mathcal{O}(C(f,P)f^2\log f)$ where P is the number of incident angles considered. Moreover MLFMM significantly reduces the memory footprint, which removes the need for very advanced hardware. It is especially effective when combined with higher-order basis functions that can reduce the number of unknowns for a specific frequency [6]. However, even with these improvements, the runtimes still depends on the number of iterations $C(f,P)$ required to solve the linear system that arises with an iterative solver for all incident angles. The computational effort for iterative solvers will scale with P, in contrast to direct solvers, where a factorization can be reused for all Right Hand Sides (RHS). To tackle this issue [5] utilize interpolation techniques to reduce the number of RHS of the linear system compared to the number of incident angles requested by the user. This relies on using a sampling criterion to determine how many RHS are required to accurately represent the RCS.

In this paper we will also use higher-order basis functions and MLFMM. But instead of using interpolation we will compress the RHS matrix arising from the incident angles algebraically. This is possible due to the fact that for incident angles close to one another, the RHS matrix has low numerical rank. It has the advantage that we can avoid the interpolation step from [5] and directly compress the matrix arising from the incident angles provided by the user. Additionally we demonstrate that this compression can reduce the number of RHS significantly even compared to the criterion in [5]. This is of benefit both with regards to the runtime and the memory footprint of the algorithm.

Combining higher-order basis functions and a blocked iterative solver we demonstrate that the proposed method can efficiently compute the monostatic RCS of complex and electrically large structures without utilizing advanced hardware.

II. Monostatic Radar Cross Section

In a given direction (θ_u, ϕ_u) the radar cross section $\sigma(\theta_u, \phi_u)$ of a structure is generally defined as [7, p. 64]

$$\sigma(\theta_u,\phi_u) = \lim_{r\to\infty} 4\pi r^2 \frac{|\boldsymbol{E}^S(\theta_u,\phi_u)|^2}{|\boldsymbol{E}^I(\theta_i,\phi_i)|^2}. \tag{1}$$

Here $\boldsymbol{E}^I(\theta_i,\phi_i) = \boldsymbol{E}_0 e^{-jk_0\hat{\boldsymbol{k}}\cdot\bar{r}}$ is the incident electric field due to a plane-wave with amplitude $\boldsymbol{E}_0$, propagation vector $\hat{\boldsymbol{k}} = -(\sin\theta_i\cos\phi_i\hat{\boldsymbol{x}} + \sin\theta_i\sin\phi_i\hat{\boldsymbol{y}} + \cos\theta_i\hat{\boldsymbol{z}})$ and the free-space wavenumber k_0. $\boldsymbol{E}^S(\theta_u,\phi_u)$ is the scattered far field in direction (θ_u,ϕ_u).

Taking into account the polarization of the incident and scattered fields we define the $\hat{\boldsymbol{\psi}}$-polarized RCS for a $\hat{\boldsymbol{\nu}}$-polarized incident field as

$$\sigma(\theta_u,\phi_u)_{\psi\nu} = \lim_{r\to\infty} 4\pi r^2 \frac{|\boldsymbol{E}^S(\theta_u,\phi_u)\cdot\hat{\boldsymbol{\psi}}|^2}{|\boldsymbol{E}^I_{\hat{\boldsymbol{\nu}}}(\theta_i,\phi_i)|^2}. \tag{2}$$

Here $\boldsymbol{E}^I_{\hat{\boldsymbol{\nu}}}(\theta_i,\phi_i)$ is the electric field due to a $\boldsymbol{\nu}$-polarized plane-wave from the direction (θ_i,ϕ_i). Commonly the polarization vectors are chosen as the spherical unit vectors such that $\hat{\boldsymbol{\psi}},\hat{\boldsymbol{\nu}} = \hat{\boldsymbol{\theta}},\hat{\boldsymbol{\phi}}$.

III. Solution strategy

Our solution strategy consists of several different building blocks that each contributes to the performance for electrically large structures. It can be outlined as follows.

We will consider an integral equation formulation, discretized using the method of moments. This requires solving a large linear system, which is the bottleneck of the computational effort. To reduce this bottleneck we use an acceleration method, the MLFMM, and employ higher-order basis functions to decrease the number of unknowns. The potentially large number of RHS still remains a challenge, which motivates the use of a compression of the RHS. Finally we utilize a blocked iterative solver to further reduce the number of matrix-vector products that is required.

A. Integral Equations and Discretization

To solve the full-wave problem we consider integral equations for time harmonic waves and perfectly electrical conducting scatterer $\mathcal{S}$. The integral equations can be expressed as a mixed potential Electric Field Integral Equation (EFIE), however for closed parts of $\mathcal{S}$ we employ the Combined Field Integral Equation (CFIE) to avoid internal resonance. We note that homogeneous dielectric scatterers can be considered with the Poggio-Miller-Chang-Harrington-Wu-Tsai (PMCHWT) formulation [8]. Using a Galerkin approach to discretize the equations we arrive at a system of linear equations

$$\overline{\overline{Z}}\,\overline{\overline{I}} = \overline{\overline{V}}. \tag{3}$$

Here $\overline{\overline{Z}}$ is called the impedance matrix and is of size $N \times N$. The matrix $\overline{\overline{V}}$ contains the RHS and is of size $N \times P$. Finally $\overline{\overline{I}}$ is also of size $N \times P$.

When considering just one polarization, the number of RHS, P, is equal to the number of incident angles considered in the monostatic RCS.

The system of equations (3) can either be solved with a direct solver requiring $\mathcal{O}(N^3 + N^2 P)$ operations or with an iterative solver requiring $\mathcal{O}(C(f,P)N^2)$.

B. Multi-Level Fast Multipole Method and Higher-Order Basis Functions

As using the Method of Moments (MoM) requires $\mathcal{O}(N^2)$ operations it becomes intractable for electrically large structures. To remedy this we will use MLFMM which reduces the number of required operations to $\mathcal{O}(C(f,P)N\log N)$. To further reduce the computational cost we use higher-order basis functions to reduce the number of unknowns significantly compared to using the RWG basis functions.

While using MLFMM instead of MoM will certainly reduce the memory footprint, it is still not clear whether the runtime will actually be reduced, as this will depend on $C(f,P)$. Given the number of RHS P we can estimate $C(f,P)$ as

$$C(f,P) = N_{it} P \tag{4}$$

where N_{it} is the number if iterations of an iterative solver to solve for one right hand side. This shows that the number of right hand sides are crucially important to the performance of MLFMM.

C. Compression of Right Hand Sides

In order to improve on the scaling given in (4) we will in this work apply compression to the RHS, $\overline{\overline{V}}$, in order to reduce the number of iterations $C(f,P)$ compared to (4).

The compression relies on the observation that for two incidence angles close to each other the currents induced on $\mathcal{S}$ are similar. This translates into the fact that the two corresponding columns of $\overline{\overline{V}}$ will be almost linearly dependent. So as long as we sample close enough we should expect $\overline{\overline{V}}$ to have numerical rank k such that $k < P$.

This can be exploited by writing $\overline{\overline{V}}$ as a matrix product

$$\overline{\overline{V}} \approx \overline{\overline{C}}\,\overline{\overline{D}}, \tag{5}$$

where $\overline{\overline{C}}$ is of size $N \times k$ and $\overline{\overline{D}}$ is of size $k \times P$. We can now solve the linear system

$$\overline{\overline{Z}}\,\overline{\overline{X}} = \overline{\overline{C}}, \tag{6}$$

and use $\overline{\overline{D}}$ to recover an approximation to $\overline{\overline{I}}$ as

$$\overline{\overline{I}} \approx \overline{\overline{X}}\,\overline{\overline{D}} \tag{7}$$

If k, $\overline{\overline{C}}$ and $\overline{\overline{D}}$ are chosen appropriately then the approximation error $E = \|\overline{\overline{I}} - \overline{\overline{X}}\,\overline{\overline{D}}\|$ can be controlled.

As a benchmark for our compression we will consider the number of right hand sides based on the sampling criterion from [5], [9]

$$P_{\text{sc}} = \frac{\phi_{\text{int}}}{\Delta\phi} = \frac{4f\rho_{\max}\phi_{\text{int}}}{c_0}. \tag{8}$$

Here c_0 is the speed of light and $\rho_{\max}$ is the maximum object radius in the observation plane. We note that P_{sc} is the number of right-hand sides for each polarization of the incident plane wave. P_{sc} can be seen as the number of right hand sides we had to use if we were to use interpolation as in [5] instead of the compression.

D. Iterative Solver

The most popular solver for MLFMM is GMRES [10] which is a Krylov solver that, in its basic formulation, treats each right hand side independently. Hence, in its basic formulation no information from the solution of one right hand side is reused for the solution of another right hand side, aside from possibly reusing the last solution as an improved starting guess. To improve on this we use the Block-GMRES from [11]. Rather than minimizing the residual $\overline{r} = \overline{\overline{Z}}\,\overline{I} - \overline{V}$ over the Krylov space $\{\overline{r}, \overline{\overline{Z}}\,\overline{r}, \overline{\overline{Z}}^2\,\overline{r}, \ldots\}$, the Block-GMRES minimizes all P residuals $\overline{\overline{R}} = \overline{\overline{Z}}\,\overline{\overline{I}} - \overline{\overline{V}}$ simultaneously over the Krylov space $\{\overline{\overline{R}}, \overline{\overline{Z}}\,\overline{\overline{R}}, \overline{\overline{Z}}^2\overline{\overline{R}}, \ldots\}$. This can reduce the number of matrix-vector products compared to the estimate given in (4) [12].

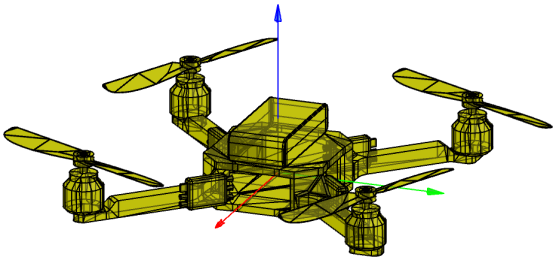

Fig. 1. The MoM mesh for the delivery drone discussed in Section IV-A. The red arrow indicates the x-direction, the green the y-direction and the blue the z-direction.

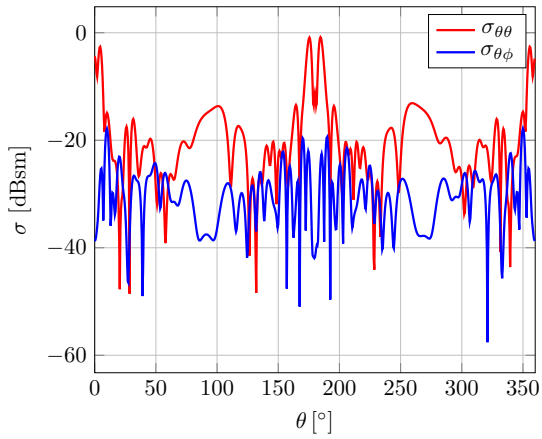

Fig. 2. Monostatic RCS for the delivery drone discussed in Section IV-A for a full spherical cut for $\phi = 0$.

IV. Results

In this section we will demonstrate our approach by computing the monostatic RCS for three different applications. As previously we let P denote the total number of incident angles given by the user, and we let $P_{\text{c}} = k$ denote the number of RHS after compression. While the three cases all demonstrates the method on real world problems, they also illustrate three different aspects of the performance. In the case IV-A we show how we are able to compress to a number of right hand sides lower that the criterion given in (8). In the case IV-B we show how our approach lets us compute the RCS for a grid of directions (θ_i, ϕ_i), that leads to a very large number of incident angles. Finally the last case IV-C illustrates that the method can be applied to electrical large structures. We emphasize that all the results are generated on a laptop, with an i7 2.7 GHz with 12 cores and 32GB of memory.

A. Delivery Drone

As the first example we consider a delivery drone shown in Figure 1. The data and results are shown in Table I. The RCS for $P = 720$ number of incident angles is plotted in Figure 2. As seen in Table I the number of right hand sides is compressed to $P_{\text{c}} = 52$ which is significantly lower than the estimated number of right hand sides by the criterion in (8).

The Monostatic RCS is plotted in Figure 2.

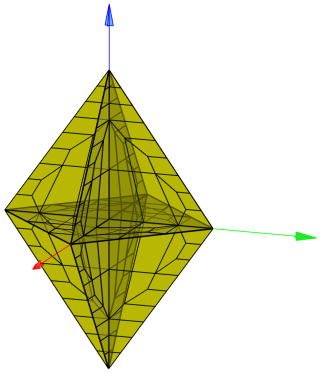

Fig. 3. The MoM mesh for the corner reflector discussed in Section IV-B. The red arrow indicates the x-direction, the green the y-direction and the blue the z-direction.

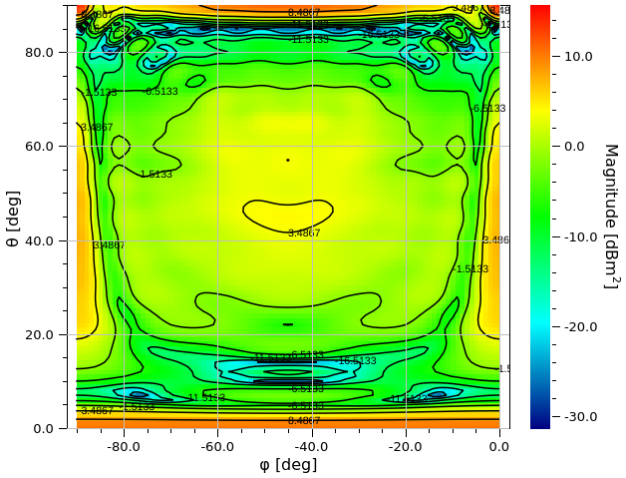

Fig. 4. The RCS grid for the corner reflector discussed in Section IV-B.

B. Corner Reflector

For the second case we consider the triangular corner reflector shown in Figure 3. For this case we compute the RCS for a grid of incident directions, to demonstrate that the compression is effective for large problems. We consider $91 \times 91 = 8281$ grid points. As seen from the results in Table I the number of right hand sides after the compression is only $P_{\text{c}} = 180$, which amounts to a compression to less than 2.5% of the initial number of right hand sides.

The RCS grid is shown in Figure 4.

C. Helicopter

The final case we consider is an electrically large helicopter of size shown in Figure 5. We consider a frequency of 8 GHz and the helicopter has a radius of $\rho_{\max} = 93.4\lambda$, so this is an electrically large problem. The computed RCS is shown in Figure 6. Even with the highly varying RCS we were still able to compress the right hand sides to around $\frac{1}{3}$ of the number of right hand sides necessary according to the criterion (8).

TABLE I

RESULTS FOR THE FULL-WAVE RCS COMPUTATION OF THE THREE CASES. THEY WERE ALL RUNNED ON A LAPTOP, WITH AN I7 2.7 GHZ WITH 12 CORES AND 32GB OF MEMORY. f DENOTES THE FREQUENCY, $\rho_{\max}$ THE RADIUS OF THE MINIMUM ENCLOSING SPHERE, N THE NUMBER OF UNKNOWNS, P THE NUMBER OF RHS, P_{sc} THE REQUIRED NUMBER OF RHS ACCORDING TO THE CRITERION (4) AND P_{c} THE NUMBER OF RHS AFTER COMPRESSION.

Case	f	$\rho_{\max}$	N	P	P_{sc}	P_{c}	Run time
Delivery Drone	10 GHz	0.16 m	10325	720	135	52	3 min
Corner Reflector	8 GHz	0.21 m	14452	8281	-	180	9:44 min
Helicopter	8 GHz	3.5m	333479	1173	1173	392	8:44 hours

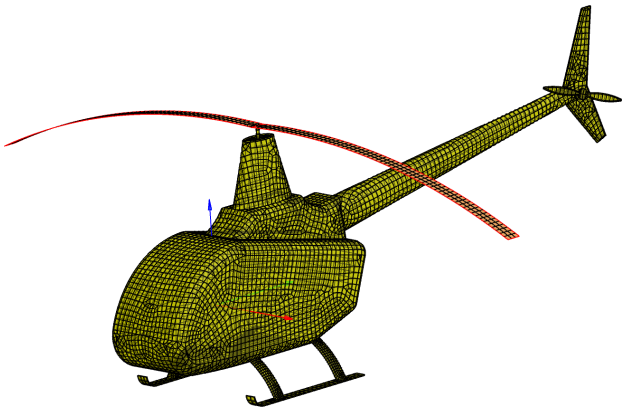

Fig. 5. Mesh of helicopter at discussed in Section IV-C. The red arrow indicates the x-direction, the green the y-direction and the blue the z-direction.

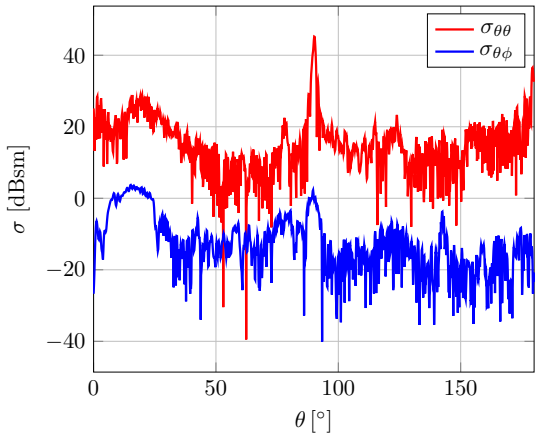

Fig. 6. Monostatic RCS for the helicopter discussed in Section IV-C for a full spherical cut for $\phi = 0$.

V. CONCLUSION

It was demonstrated that MLFMM with higher-order basis functions in combination with a compression of the right hand side matrix allows for efficiently computing the monostatic RCS of electrically large structures, without requiring advanced hardware. The implementation of this approach was shown to provide a strong performance for a number of different cases.

REFERENCES

[1] Y. An, D. Wang, and R. Chen, "Improved multilevel physical optics algorithm for fast computation of monostatic radar cross section," *IET Microwaves, Antennas & Propagation*, vol. 8, pp. 93–98, Jan. 2014.

[2] K. Divyabramham and R. Vulapalli. RCS Predictions for Electrically Large Complex Structures. [Online]. Available: https://goo.gl/81QH5X

[3] M. S. Pavlovic, M. S. Tasic, B. L. Mrdakovic, and B. M. Kolundžija, "WIPL-D: Monostatic RCS Analysis of Fighter aircrafts," in *EuCAP 2016*. IEEE, Nov. 2016.

[4] G. Cakir, M. Cakir, and L. Sevgi, "Radar Cross Section (RCS) Modeling and Simulation, Part 2: A Novel FDTD-Based RCS Prediction Virtual Tool for the Resonance Regime," *IEEE Antennas and Propagation Magazine*, vol. 50, no. 2, pp. 81–94, Apr. 2008.

[5] O. Borries, E. Jørgensen, and P. Meincke, "Monostatic RCS Analysis of Electrically Large Structures using Integral Equations," in *European Conference on Antennas and Propagation*, Mar. 2017.

[6] O. Borries, P. Meincke, E. Jørgensen, and P. C. Hansen, "Multilevel Fast Multipole Method for Higher-Order Discretizations," *IEEE Transactions on Antennas and Propagation*, vol. 62, no. 9, pp. 4695–4705, Sep. 2014.

[7] E. F. Knott, J. Shaeffer, and M. Tuley, *Radar Cross Section*, 2nd ed. SciTech Publishing, Aug. 2004.

[8] A. J. Poggio and E. K. Miller, "Integral equation solution of three-dimensional scattering problems." in *Computer Techniques for Electromagnetics*, R. Mittra, Ed. New York: Pergamon Press, Inc, 1973, pp. 159–264.

[9] H. Buddendick and T. F. Eibert, "Acceleration of Ray-Based Radar Cross Section Predictions Using Monostatic-Bistatic Equivalence," *IEEE Trans. Antennas Propag.*, vol. 58, no. 2, pp. 531–539, Jan. 2010.

[10] Y. Saad and M. H. Schultz, "GMRES: A Generalized Minimal Residual Algorithm for Solving Nonsymmetric Linear Systems," *SIAM J. Sci. Comput.*, vol. 7, no. 3, pp. 856–869, Jun. 1986.

[11] M. H. Gutknecht, "Block Krylov space methods for linear systems with multiple right-hand sides: an introduction," *Seminar for Applied Mathematics*, 2006.

[12] H. Calandra, S. Gratton, J. Langou, and X. Pinel, "Flexible variants of block restarted GMRES methods with application to geophysics," *SIAM Journal on Scientific Computing*, 2012.